Proceedings of the Canadian Society for Mechanical Engineering International Congress
Computational Fluid Dynamics Canada International Congress
CSME - CFD-SC2023
May 28-31, 2023, Sherbrooke, QC, Canada

An experimental study of buoyant jets: effects of viscoplasticity

Mir Hedayat Moosavi, Hossein Hassanzadeh, Soheil Akbari, Seyed Mohammad Taghavi*
Department of Chemical Engineering, Université Laval, Québec, Canada G1V 0A6
*e-mail: seyed-mohammad.taghavi@gch.ulaval.ca

Abstract—In this paper, we experimentally investigated the injection of a Newtonian jet into Newtonian/viscoplastic ambient fluids. Although this study has applications in environmental flows, mixing processes, and so on, the main application of our interest is the plug and abandonment of oil and gas wells. Hence, we analyzed the impingement time of the jet in addition to other jet characteristics, namely, the laminar length and the deviation length. Furthermore, we observed two regimes for different ambient fluids, i.e. the mixing regime for a Newtonian ambient fluid and the trapped regime for a viscoplastic ambient fluid. Moreover, we examined the impact of the Reynolds number (*Re*) and the Bingham number (B_N), on the jet characteristics. *Re* and B_N have opposite effects on the impingement time, causing a decrease and growth, respectively. We also observed the existence of a laminar length at higher *Re* in the trapped regime, compared to the mixing regime. An increase in *Re* results in a growth in the deviation length for both regimes, and this growing trend is more drastic for the mixing regime.

Keywords-Buoyant jets; Jet flow regimes; Miscible fluids; Viscoplastic fluid

I. INTRODUCTION

Miscible/immiscible negatively and positively buoyant jets have been the subject of several studies [1-5]. In contrast to negatively buoyant jets, buoyancy and momentum fluxes for positively buoyant jets act in the same direction [6]. Two-phase fluids that are miscible or immiscible have been investigated for a long time in many areas, in other relevant injection flow contexts, such as displacement flows [7-10]. Depending on whether there is interfacial tension between the fluids, either a miscible or an immiscible jet can be produced [11].

The present study is motivated by the application of jet cleaning in the plug and abandonment (P&A) process of oil and gas wells, a critical operation aimed at preventing contamination of groundwater and spills from offshore wellbores through the use of a cement plug [12, 13]. After the cessation of its operational lifespan, a well must be thoroughly sealed and decommissioned to avoid the potential for uncontrolled leaks that may harm fragile marine habitats [12, 13]. A common method for achieving this is to inject a cement slurry into the wellbore, which subsequently dries and acts as a solid barrier [14, 15]. In preparing the well for the placement of a cement plug, the clearance of the site is a crucial aspect of P&A operations, for which the jet cleaning technique has been developed as a recent innovation [6]. Hassanzadeh *et al.* conducted an experimental investigation of a buoyant, vertical, miscible jet flow, analyzing various quasi-steady features including laminar length, jet radius, spread angle, virtual origin, velocity profiles, and energy dissipation [6]. In a separate study of vertical jets, they identified three flow regimes - a jellyfish regime, a funnel regime, and a cone regime - and examined the impact of a viscosity ratio (*m*) on the flow behaviors of their buoyant jets [16].

Numerous studies have examined various types of horizontal, angled, buoyant, and non-buoyant jets, in relation to the wide range of applications, including gaseous jets used in aeration processes [17], solid rocket motors operating underwater [18], hydrogen safety [19], industrial smelting processes [20], coastal sewage disposal projects [21], and others. Arakeri *et al.* [22] tested a horizontally discharged laminar buoyant jet to investigate bifurcations. They conducted experiments and recorded their findings based on the injection of clean water into a brine solution. They discovered that bifurcation was a phenomenon that occurred in high Schmidt (*Sc*) or high Prandtl (*Pr*) number jets and that it was brought on by the slower-moving fluid flowing nearer the edge of the jet. Hammad [23] numerically analyzed the flow and decay properties of submerged jets of shear-thinning fluids under yield stress. Using a finite difference method, they were able to derive numerical solutions to the governing mass and momentum conservation equations, using the Herschel-Bulkley rheological model. They conducted a parametric analysis to look at the impact of flow inertia and rheology. According to their findings, the momentum and velocity penetration depths of submerged jets are dramatically reduced when yield stress is present.

Although numerous studies have been conducted in the submerged jet area, there is a lack of proper coverage on jetting a Newtonian fluid into a non-Newtonian ambient fluid. In this context, in this paper, we experimentally investigate a horizontal buoyant jet of brine solution in both Newtonian and non-Newtonian ambient fluids. We aim to analyze the effects of the jet velocity, the viscosity of the ambient fluid, and buoyancy on the jet characteristics. In the following sections, we first explain our experimental setup and procedure. We then discuss the parameters and characteristics of interest in this paper. Then, we present our results and discuss them.

II. EXPERIMENTS

A. Experimental setup and procedure

In order to produce a buoyant miscible jet, we injected a solution of salt water as a heavy fluid using a gear pump (ISMATEC MCP-Z Standard) into a light ambient fluid (i.e. deionized water/Carbopol gel, with a density equal to that of water. A digital rheometer (DHR-3, TA Instruments) was used to measure the rheological properties of our Carbopol gel. In Table 1, the parameters determined from the rheological measurements of our ambient fluids are presented. Using a high-speed digital camera (Basler aca2040-90um), we captured experimental side-view images of the jet at a rate of 20 frames per second. Fig. 1 shows the schematic of our setup. The Newtonian jet fluid (black fluid), which was injected into the tank of deionized water in Fig. 2, is an example of the Newtonian jet in our study. Also, some of the characteristics considered in this paper can be seen in this figure. Using an in-house MATLAB code, the calibrations of the light absorption and picture processing were carried out. With values ranging between the normalized values of 0 and 1, for the pure jet and pure ambient fluids, respectively, the calibrated pictures were converted into concentration maps.

TABLE I. PARAMETERS DETERMINED FROM THE RHEOLOGICAL MEASUREMENTS OF AMBIENT FLUIDS.

Sample	$\hat{\tau}_y$ **(Pa)**	$\hat{k}$ **(Pa.s^n)**	**n**
Deionized water	0	0.001	1
Carbopol gel	0.1778	0.1727	0.6628

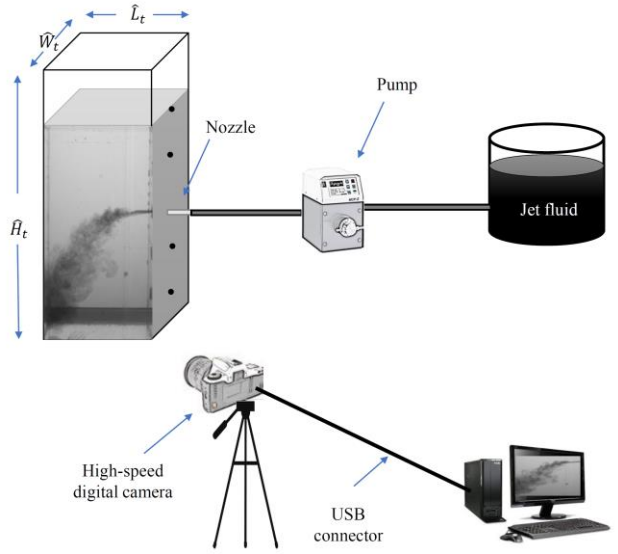

Figure 1. Schematic of our experimental setup.

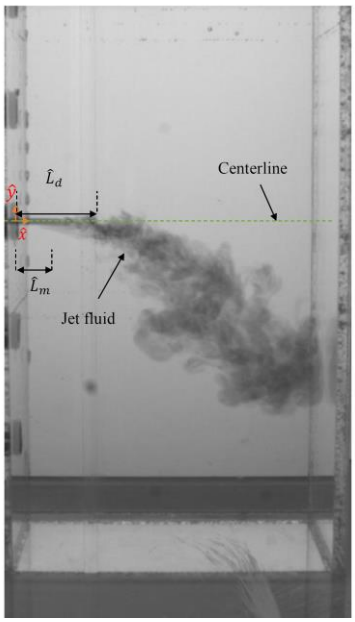

Figure 2. A typical horizontal Newtonian jet in our experiments. The laminar region and the distributed region are the two primary parts of the jet, respectively. Laminar length, $\hat{L}_m$, refers to the steady, non-mixing portion of the jet and is the length of the laminar zone. Additionally, the deviation length, $\hat{L}_d$, is described as the distance between the deviation point of the jet trajectory and the nozzle's horizontal plane.

B. Scope of experiments

In this paper, we inject a jet fluid into an ambient fluid after passing through a nozzle. The mean injection velocity in the horizontal plane is $\hat{V}_{j,0}$, and the nozzle has a circular cross-sectional area. The fluids have various densities ($\hat{\rho}_j \geq \hat{\rho}_a$) and they are miscible. In this work, we adhere to the convention that dimensional quantities are denoted by the symbol "^" whereas dimensionless quantities are not. The properties of the jet fluid and ambient fluid, respectively, are also denoted by the subscripts j and a. Table 2 presents the rectangular tank dimensions as well as the scope of the dimensional flow characteristics.

Our flow is governed by at least eight dimensionless numbers, according to the Buckingham's Pi theorem, as shown in Table 3. Some of these, however, are fixed or have no bearing on our work. First, because *Pe* has very big values (*Pe*>>1), its effect is disregarded. Second, because our density differences in our tests fall within the Boussinesq approximation's range (*At*<<1), the Atwood number (*At)* is not a crucial flow parameter. In our investigation, all the geometrically dimensionless numbers (i.e. δ_1, δ_2, δ_3) are fixed. When defining the viscosity ratio, which is the ratio of the effective viscosity of the ambient fluid to the viscosity of the jet fluid, we also take into account the power-law index (*n*). Thus, the remaining dimensionless numbers, such as the Reynolds number (*Re*), the Bingham number (B_N), and the Froude number (*Fr*), may be assumed to govern our jet flows.

We use the characteristic time scale (1) and the characteristic length (2) to generalize our results, by rendering all the lengths, and times dimensionless:

$$\hat{L}_Q = \frac{\hat{Q}_0}{\hat{M}_0^{1/2}} \sim \hat{D}_n \quad (1)$$

$$\hat{t}_Q = \frac{\hat{Q}_0^{2}}{\hat{M}_0^{3/2}} \sim \frac{\hat{D}_n}{\hat{V}_{j,0}} \quad (2)$$

TABLE II. RECTANGULAR TANK DIMENSIONS AND THE SCOPE OF DIMENSIONAL CHARACTERISTICS.

Parameter	Name	SI units	Range or value
$\hat{D}_m$	Molecular diffusivity	m^2/s	2×10^{-9}
$\hat{D}_n$	Nozzle diameter	m	3.6×10^{-3}
$\hat{L}_t$	Distance between nozzle and tank end-wall	m	1.3×10^{-1}
$\hat{H}_t$	Height of tank	m	3×10^{-1}
$\hat{W}_t$	Width of tank	m	1×10^{-1}
$\hat{V}_{j,0}$	Injection mean velocity	m/s	$(3.28 - 22.94) \times 10^{-1}$
$\hat{\mu}_a$	Viscosity of ambient fluid	Pa. s	$(1 - 39) \times 10^{-3}$
$\hat{\mu}_j$	Jet fluid's viscosity	Pa. s	1×10^{-3}
$\hat{\rho}_a$	Ambient fluid's density	Kg/m^3	9.98×10^2
$\hat{\rho}_j$	Jet fluid's density	Kg/m^3	10.5×10^2

TABLE III. DEFINITIONS AND RANGES OF DIMENSIONLESS PARAMETERS USED IN THIS STUDY.

Parameter	Name	Definition	Range
At	Atwood number	$\frac{\hat{\rho}_j - \hat{\rho}_a}{\hat{\rho}_j + \hat{\rho}_a}$	2.59×10^{-2}
Fr	Froude number	$\frac{\hat{V}_{j,0}}{\sqrt{At\hat{g}\hat{D}_n}}$	$(1.083 - 7.586) \times 10$
m	Viscosity ratio	$\frac{\hat{\mu}_a}{\hat{\mu}_j}$	1-39
Pe	Peclet number	$\frac{\hat{V}_{j,0}\hat{D}_n}{\hat{D}_m}$	$(0.2 - 1.7) \times 10^6$
B_N	Bingham	$\frac{\hat{\tau}_{y_a}}{\hat{k}_a(\hat{V}_{j,0}/\hat{D}_n)^n}$	$(0 - 5.2) \times 10^{-2}$
Re	Reynolds number	$\frac{\left(\left(\hat{\rho}_a + \hat{\rho}_j\right)/2\right) \times \hat{V}_{j,0} \times \hat{D}_n}{\hat{\mu}_j}$	$(1.2 - 8.4) \times 10^3$
δ_1	Aspect ratio 1	$\frac{\hat{L}_t}{\hat{D}_n}$	3.6×10
δ_2	Aspect ratio 2	$\frac{\hat{H}_t}{\hat{D}_n}$	8.3×10
δ_3	Aspect ratio 3	$\frac{\hat{W}_t}{\hat{D}_n}$	2.8×10

III. RESULTS AND DISCUSSIONS

The key experimental results for a given range of flow parameters are presented in this section. Our results reveal that two jet flow patterns are formed when using either a Newtonian ambient fluid or a viscoplastic ambient fluid, namely, the mixing regime and the trapped regime, respectively. Fig. 3 and Fig. 4 illustrate the snapshots and the spatiotemporal concentration diagram, respectively, for one example test for each regime. It should be noticed that the amount of the jet fluid's existence at each distinct dimensionless point, *x*, and dimensionless time, *t*, is indicated by the darker zone. As can be seen in Fig. 4a after $t \approx 270$, when the impingement happens, the concentration of the jet fluid surges, showing the turning back-flow of the jet. Moreover, a glance at Fig. 4b reveals that in the trapped regime there is much less mixing and most of the tank space is covered with the pure ambient fluid only. Also, it can be observed that at $t \approx 230$ the jet penetration almost stops, the jet front falls down, and as a result, at $x \approx 20$ we observe a thin, dark area indicating a high concentration of the jet fluid.

The impingement time, defined as the time when the jet fluid front reaches the end wall, is illustrated in Fig. 5. In Fig. 5a the dimensional impingement time for both regimes is illustrated. As can be seen, increasing the jet velocity, resulting in increasing *Re*, decreases the dimensional impingement time. Also, it can be seen that in the trapped regime, as a result of the presence of the viscoplastic ambient fluid, the impingement does not happen until *Re* reaches a value of around 3000. As the Reynolds number increases, the inertia force becomes more dominant and it governs the penetration of the jet fluid; as a result, the difference between impingement times of two regimes is reduced. In addition, Fig. 5b, which presents the dimensionless impingement time in terms of B_N, depicts that increasing B_N causes an overall trend of increasing the impingement time. The occurrence of this phenomenon is attributed to the yield stress of the viscoplastic ambient fluid, which hinders the jet penetration.

We define/consider the maximum length of the jet where the jet radius is still equal to the radius of the nozzle as the laminar length. Accordingly, we presented this characteristic in Fig. 6. In the first case of the mixing regime in our experiments (Re≈1200) we observe bifurcation, which is in accordance with the bifurcation range reported by Arakeri *et al.* [22]. In this case, we reported the laminar length as the distance between the nozzle and the point where the turbulent region begins and the jet becomes unstable, although we can see a secondary plume at this distance.

As can be seen from Fig .6a, increasing *Re* causes a drop in the laminar length, up to a point where the jet becomes fully turbulent and the laminar length disappears at *Re*≈3000 for the mixing regime and at *Re*≈4800 for the trapped regime. This figure also reveals that, in our viscoplastic ambient fluid, by increasing B_N, the jet becomes more stable; this is more obvious in Fig. 6b, which illustrates the laminar length for the trapped regime in terms of B_N. In Fig. 6a, we rely on the following correlation:

$$L_m \approx 324.4(Ar^{0.29} + 38.6)Re^{-1}, \quad (3)$$

introduced by Hassanzadeh *et al.* [6] for the purpose of comparisons. The fact that the data points are below the correlation line suggests that correlation (3) tends to overpredict the experimental data, as can be seen from the graph. This discrepancy may be expected given that correlation (3) was developed under an infinite environment assumption (i.e. a free jet); however, in the current investigation, the wall's potential impact (especially the impingement wall) can be significant, and in comparison with an infinite environment, a bounded domain may cause more turbulence [24].

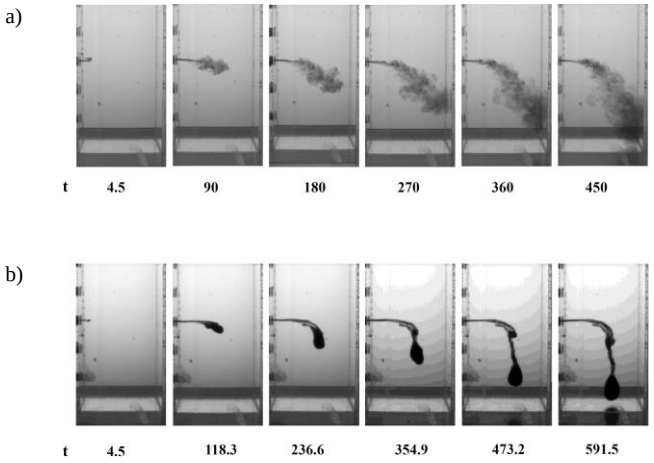

Figure 3. Sequence of experimental snapshots of a) the mixing regime ($Re\approx$ 1200, B_N=0), b) the trapped regime ($Re\approx$1200, $B_N\approx$0.052).

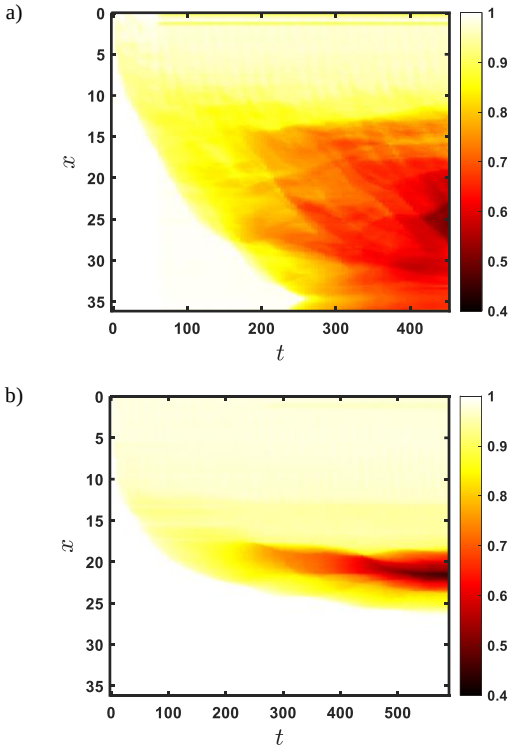

Figure 4. The spatiotemporal concentration diagram a) the mixing regime ($Re\approx$ 1200, B_N=0), b) the trapped regime ($Re\approx$1200, $B_N\approx$0.052).

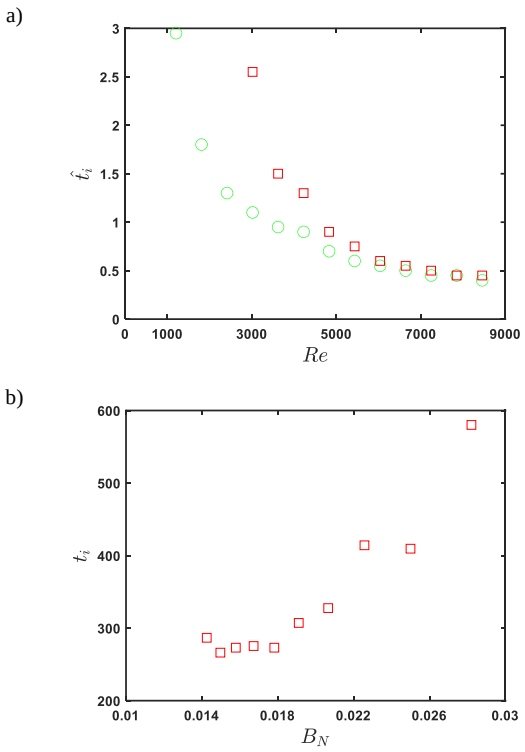

Figure 5. a) Variation of the dimensional impingement time for the mixing regime (green circles) and the trapped regime (red squares) versus *Re*, b) Variation of the dimensionless impingement time for the trapped regime versus B_N.

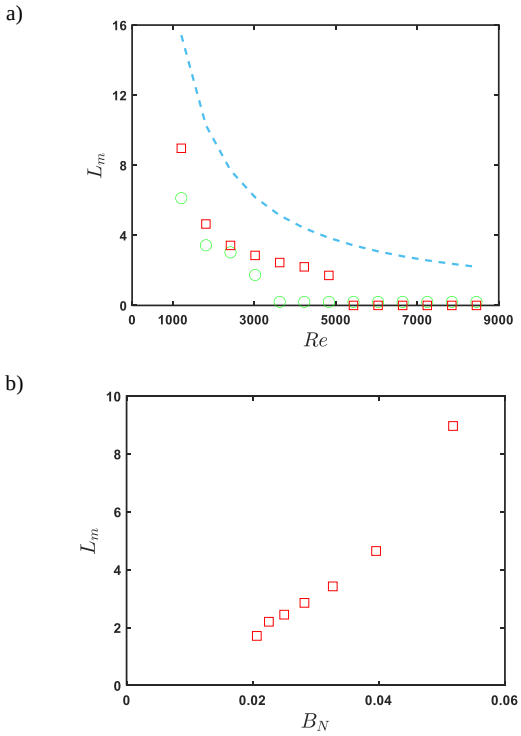

Figure 6. a) Variation of the dimensionless laminar length for the mixing regime (green circles) and the trapped regime (red squares) compared to the correlation (blue line) versus *Re*. b) Variation of the dimensionless laminar length for the trapped regime, in terms of B_N.

Let us define another characteristic named the "deviation length," as can be seen from Fig. 2, corresponding to the length where the jet trajectory starts to deviate from the horizontal plane of the nozzle. Fig. 7 shows the deviation length for both regimes (until the point that the jet impinges before it can deviate). It can be observed from Fig. 7 that, at low *Re*, the deviation length for the Newtonian ambient fluid is lower than that for the viscoplastic ambient fluid. However, at $Re \approx 2400$ inertia is the most important force for the mixing regime, and it overcomes the buoyancy and moves the deviation length forward until $Re \approx 3000$ where the jet impinges before it can deviate. On the other hand, the yield stress of the ambient fluid hinders the inertia force in the trapped regime, and as a result for higher *Re* (up to 3600), the buoyant jet deviates before reaching the end wall of the tank. By comparing our results for the mixing regime with the results of Alfaifi *et al.* [25], we can see that since they had considerably lower density differences between the jet and ambient fluid, they observed higher deviation lengths.

IV. Conclusion

In this paper, by carrying out an experimental study, two distinct flow regimes were observed for our miscible buoyant jets, namely, the mixing and trapped regimes. The presence/absence of these regimes is attributed to the presence/absence of the viscoplastic rheological behavior in the ambient fluids. The impact of the effective parameters, such as the injection velocity of the jet and the rheological characteristic of the ambient fluid on the jet features, was investigated by considering these parameters in their dimensionless forms, i.e., *Re* and B_N. The stabilizing influence of the viscoplastic ambient fluid on the jet regime as well as jet characteristics such as the laminar length were presented and discussed. The deviation length as a feature of the jet trajectory was introduced and the impact of *Re* on its variation was presented for both flow regimes. Further investigations for a wider range of density differences between two fluids and the viscosity of the ambient fluid are to be carried out as future work.

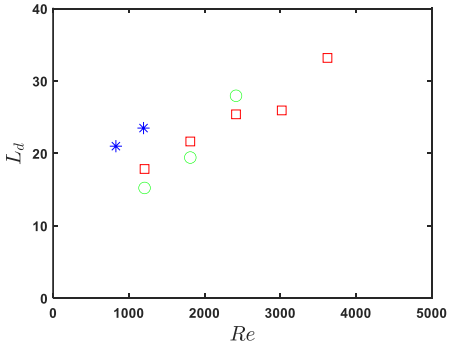

Figure 7. Variation of the deviation length for the mixing regime (green circles) and the trapped regime (red squares), and [25] (blue stars) versus *Re*.

References

[1] G. R. Hunt and N. B. Kaye, "Lazy plumes," Journal of Fluid Mechanics, vol. 533, pp. 329 – 338, 2005.

[2] A. Ezzamel, P. Salizzoni and G. R. Hunt, "Dynamical variability of axisymmetric buoyant plumes," Journal of Fluid Mechanics, vol. 765, pp. 576 – 611, 2015.

[3] A. Gharavi, A. Mohammadian, I. Nistor, E. Peña, and J. Anta, "Experimental study of surface buoyant jets in crossflow," Environmental Fluid Mechanics, vol. 20, pp.1007-1030, 2020.

[4] C.H. Lee, C. Xu, Z. Huang, "A three-phase flow simulation of local scour caused by a submerged wall jet with a water-air interface," Advances in Water Resources, vol. 129, pp.373-384, 2019.

[5] M. Hejazian, C. Darmanin, E. Balaur and B. Abbey, "Mixing and jetting analysis using continuous flow microfluidic sample delivery devices," RSC advances, vol. 10, pp.15694-15701, 2020.

[6] H. Hassanzadeh, A. Eslami, and S. M. Taghavi, "Positively buoyant jets: semiturbulent to fully turbulent regimes," Physical Review Fluids, vol..6, 054501, 2021.

[7] S.M. Taghavi, K. Alba, M. Moyers-Gonzalez and I.A. Frigaard, "Incomplete fluid–fluid displacement of yield stress fluids in near-horizontal pipes: experiments and theory," Journal of Non-Newtonian Fluid Mechanics, vol. 167, pp.59-74, 2012.

[8] M.R. Shahnazari, F. Eslami and S. Rezazadeh, "Instability analysis of miscible displacements in homogeneous porous media," Iranian Journal of Chemical Engineering, vol. 9, pp. 25-32, 2012.

[9] M. R. Shahnazari, I. Maleka Ashtiani, and A. Saberi, "Linear stability analysis and nonlinear simulation of the channeling effect on viscous fingering instability in miscible displacement," Physics of Fluids, vol. 30, 034106, 2018.

[10] M.R. Shahnazari and I.M. Ashtiani, "Investigation of viscous fingering instability in heterogeneous porous media" Special Topics & Reviews in Porous Media: An International Journal, vol. 10, pp. 15-29, 2019.

[11] D. Baumgartner, R. Bernard, B. Weigand, G. Lamanna, G. Brenn and C. Planchette, "Influence of liquid miscibility and wettability on the structures produced by drop–jet collisions," Journal of Fluid Mechanics, vol. 885, id. A23, 2020.

[12] M. Khalifeh and A. Saasen, "Introduction to permanent plug and abandonment of wells," Springer Nature, 273 p., 2020.

[13] M. Achang, L. Yanyao, and M. Radonjic, "A review of past, present, and future technologies for permanent plugging and abandonment of wellbores and restoration of subsurface geologic barriers," Environmental Engineering Science, vol. 37, pp.395-408, 2020.

[14] S. Akbari, and S.M. Taghavi, "Injection of a heavy fluid into a light fluid in a closed-end pipe," Physics of Fluids, vol. 32(6), 063302, 2020.

[15] S. Akbari, S.M. Taghavi, "Fluid experiments on the dump bailing method in the plug and abandonment of oil and gas wells," Journal of Petroleum Science and Engineering, vol. 205, 108920, 2021.

[16] H. Hassanzadeh, A. Eslami and S.M. Taghavi, "On the role of the viscosity ratio on buoyant miscible jet flows," Environmental Fluid Mechanics, vol. 22, pp. 337-365, 2022.

[17] S.K. Park and H.C. Yang, "Experimental investigation on mixed jet and mass transfer characteristics of horizontal aeration process," International Journal of Heat and Mass Transfer, vol. 113, pp. 544-555, 2017.

[18] Y. Tang and S. Li, "Research into the characteristics of horizontal gaseous jets underwater," Journal of Vibroengineering, vol. 18, pp. 4678-4691, 2016.

[19] F. Yang, T. Wang, X. Deng, J. Dang, Z. Huang, S. Hu, Y. Li and M. Ouyang, "Review on hydrogen safety issues: Incident statistics, hydrogen diffusion, and detonation process," International Journal of Hydrogen Energy, vol. 46, pp. 31467-31488, 2021.

[20] J. Ma, Y. Song, P. Zhou, W. Cheng and S. Chu, "A mathematical approach to submerged horizontal buoyant jet trajectory and a criterion for jet flow patterns," Experimental Thermal and Fluid Science, vol. 92, pp. 409-419, 2018.

[21] A. Belcaid, G. Le Palec and A. Draoui, "Numerical and experimental study of Boussinesq wall horizontal turbulent jet of fresh water in a static homogeneous environment of salt water" Journal of Hydrodynamics, vol. 27, pp. 604-615, 2015.

[22] J.H. Arakeri, D. Das and J. Srinivasan, "Bifurcation in a buoyant horizontal laminar jet," Journal of Fluid Mechanics, vol. 412, pp. 61-73, 2000.

[23] K.J. Hammad, "The flow and decay behavior of a submerged shear-thinning jet with yield stress," Journal of Fluids Engineering, vol. 138, 081205, 2016.

[24] H. Hassanzadeh, E. Cournoyer, and S.M. Taghavi, "Jet Cleaning Processes in the Plug and Abandonment of Oil and Gas Wells: An Experimental Study on Horizontal Miscible Jets," International Conference on Offshore Mechanics and Arctic Engineering, vol. 85956, V010T11A055, 2022.

[25] H. Alfaifi, A. Mohammadian, H.K. Gildeh, and A. Gharavi, "Experimental and numerical study of the characteristics of thermal and nonthermal offset buoyant jets discharged into stagnant water," Desalination and Water Treatment, vol.141, pp.171-186, 2019.